On the Use of Reverberation Chambers for Assessment of MIMO OTA Performance of Wireless Devices

(article starts on next page)

On the Use of Reverberation Chambers for Assessment of MIMO OTA Performance of Wireless Devices

Christian Lötbäck Patané, Anton Skårbratt, Robert Rehammar, Charlie Orlenius
Bluetest AB
Gothenburg, SWEDEN
{firstname.lastname}@bluetest.se

***Abstract*—The emerging of wireless MIMO enabled devices capable of reaching high data rate levels calls for new measurement methodologies for verifying the radiated performance of such devices. This paper summarizes the latest findings for a state-of-the-art MIMO OTA measurement methodology utilizing a reverberation chamber. It is shown that the reverberation chamber technique provides expected and repeatable results.**

Index Terms—MIMO; LTE; antenna measurements; reverberation chamber

I. INTRODUCTION

The increasing demand for higher data rates from end-users of wireless devices has led to the emerging of new wireless terminals based on advanced antenna systems and coding schemes. In particular, long term evolution (LTE) multiple-input multiple-output (MIMO) devices, such as handsets, tablets and USB connected data modems (dongles) are starting to reach the market. The performance of these LTE MIMO enabled devices is optimized for use in rich multipath environments, for example dense urban areas or indoor environments.

Characterization of antenna performance of wireless devices has traditionally been performed in anechoic chambers in a point-to-point sense. However, since modern wireless devices require a multipath environment to reach the intended performance enhancement, this is no longer enough. Assessment of the overall performance of multi-element antenna systems thus requires new measurement methodologies, which in some way can emulate a multipath environment.

A straightforward approach to test multi-antenna terminals is to physically emulate a multipath scattering environment, in which the performance of the device under test (DUT) is sampled. This paper describes how such a test system can be realized by utilizing the inherent properties of a reverberation chamber (RC).

The RC is today widely used and accepted for measurements of several performance parameters for wireless terminals and electrically small antennas [1, 2, 3, 4, 5]; e.g. radiation efficiency, impedance mismatch, diversity gain, MIMO capacity, total radiated power (TRP), total isotropic sensitivity (TIS) and average fading sensitivity (AFS). Its properties have been well characterized and continuously improved in order to become a very accurate over-the-air (OTA) test system [6, 7, 8, 9]. As frequently described in the literature [10, 11, 12, 13], due to the inherent multipath and Rayleigh fading characteristics of the RC, this test system also provides an ideal environment for characterization of multiple-element antenna systems with very few modifications to the test setup. Data bit throughput on the MAC or IP layer is usually used as the metric for the characterization of active MIMO terminals.

Measurement procedures for performance characterization of multi-element antenna terminals are currently extensively discussed in standardization bodies. In order to evaluate the capability of methodologies to assess the overall performance of LTE MIMO enabled devices, CTIA has developed well characterized reference antennas with known correlation and efficiency values (denoted as “Good”, “Nominal” and “Bad” antennas) [14]. This paper presents results from data bit throughput measurements of these reference antennas utilizing the RC. The results have been collected as part of a Round Robin measurement campaign arranged by CTIA during 2012 [15].

II. MEASUREMENT SETUP & PROCEDURE

Figure 1 shows the schematics of the utilized measurement setup for data bit throughput measurements in the RC. A base station simulator is connected to the fixed measurement antennas of the RC. The base station simulator is equipped with dual-ports, in order to enable MIMO signaling. The DUT is placed inside the chamber and a MIMO link is setup to the base station simulator.

An alternative measurement setup utilizes a channel emulator (CE) connected between the base station simulator and the RC. The schematics for this measurement setup can be studied in Figure 2. This setup enables testing with more advanced temporal settings, for example, additional power delay profiles or Doppler spreads other than what is inherently generated by the RC.

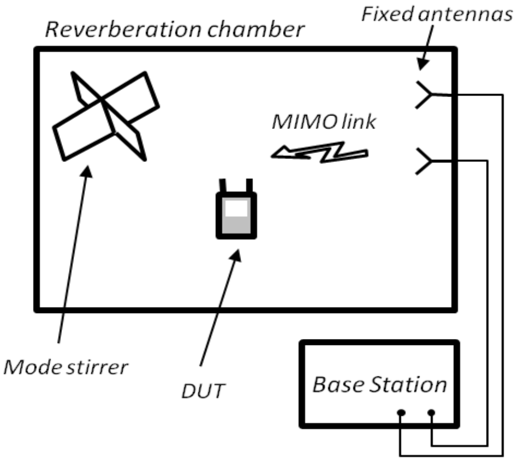

Figure 1. Basic measurement setup for data throughput measurements of MIMO enabled devices in reverberation chamber.

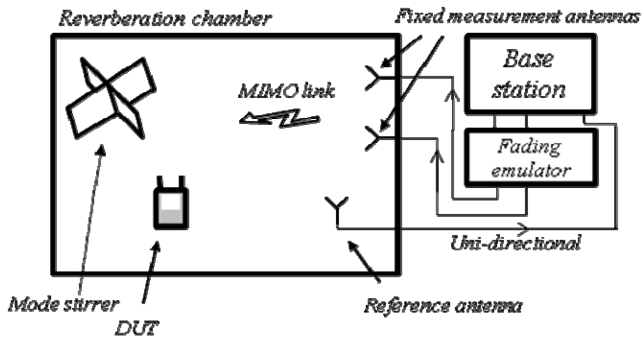

Figure 2. Measurement setup for data throughput measurements of MIMO enabled devices using a channel emulator in conjunction with a reverberation chamber.

A. Data Throughput Measurements

The procedure for data throughput measurements is based on sampling the data bit throughput for a large number of unique mode stirrer and DUT positions. During one stirring sequence a large number of subframes are transmitted by the base station simulator and the subframes acknowledged by the DUT are counted. The average cell power transmitted by the base station simulator is fixed during the stirring sequence and the average number of acknowledged subframes for a complete stirring sequence will be reported as the throughput value for that power level. This procedure is repeated for different average cell power levels and the final result will yield the throughput as a function of average available power for the DUT. In this study, a total of 40 000 subframes were used to estimate the throughput value for each power level.

III. CHANNEL EMULATION

A well-stirred RC provides a statistically isotropic Rayleigh fading environment. Thus, over a complete mode-stirring sequence, all different angle-of-arrivals of the plane waves to the DUT is equally probable and the signal amplitude exhibits a Rayleigh distribution. The power delay profile (PDP) follows an exponentially decaying function with RMS delay spreads ranging from 30 ns to 200 ns, depending on the amount of absorbing objects present inside the chamber.

For the measurements presented in this paper, the chamber was loaded with absorbing objects to achieve an inherent delay spread of 80 ns. Figure 3 shows the PDP generated by the RC during the measurements. Also, Figure 4 shows the resulting Doppler spectrum obtained in the RC due to stirrer movements. The maximum Doppler spread is only a few hertz.

When adding a CE to the setup, the spatial properties will still be the statistical isotropic channel generated inherently by the RC. However, the temporal aspects of the external channel model defined in the CE will be convolved with the inherent temporal properties of the RC. For this study, the channel emulator was programmed to emulate the temporal characteristics of the SCME urban micro and SCME urban macro channel models. Figure 5 shows the measured power delay profiles for the channel models used for these measurements. The discrete taps transmitted by the channel emulator is combined with the inherent exponential PDP of the RC given in Figure 3.

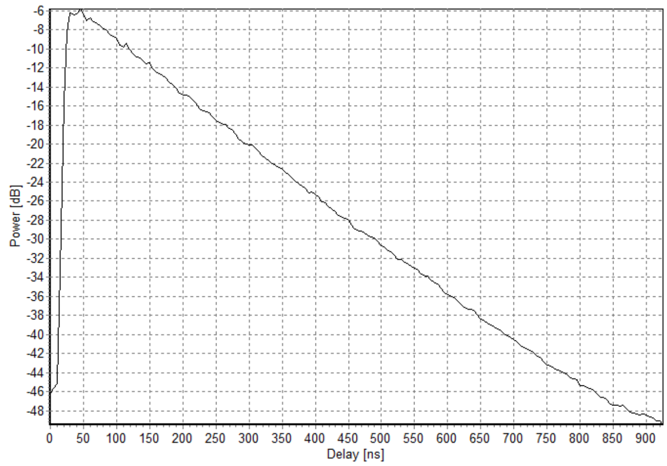

Figure 3. Measured power delay profile for the basic reverberation chamber setup.

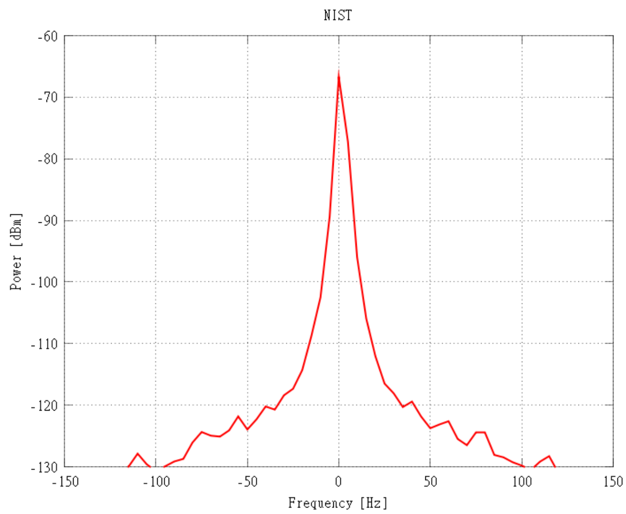

Figure 4. Measured Doppler spectrum for the basic reverberation chamber setup.

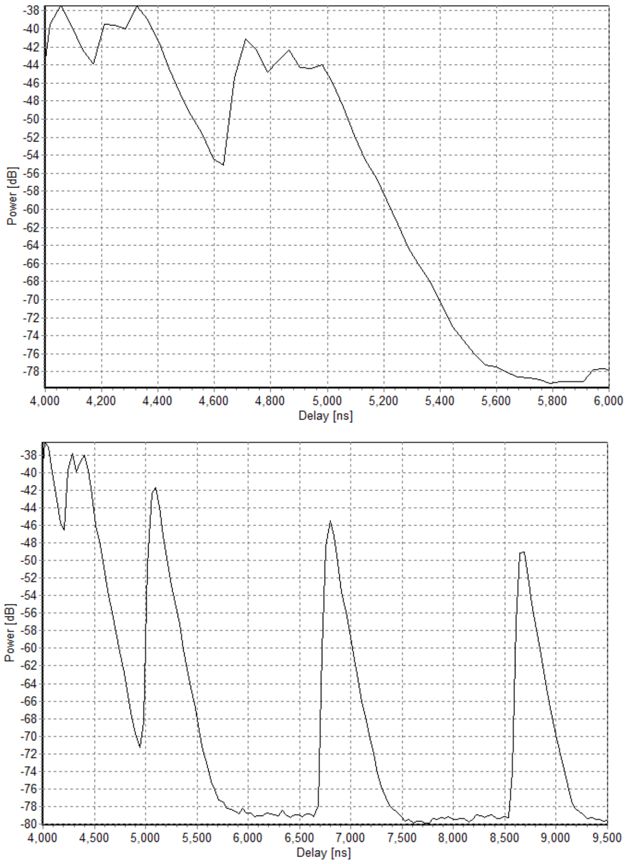

Figure 5. Measured power delay profile for the reverberation chamber and channel emulator setup. The temporal parameters for the SCME urban micro (top) and SCME urban macro channel (bottom) models were emulated bv the channel emulator.

Furthermore, Figure 6 shows the Doppler spread measured for the same emulated channel models for two different fading rates. The fading rates emulated by the channel emulator corresponded to a DUT speed of 30 km/h and 100 km/h. This gives a maximum theoretical Doppler shift of ±21 Hz and ±70 Hz respectively and aligns well with the measured maximum Doppler shift. It can be concluded that the additional effect from the stirrer movement is negligible.

IV. External Noise

External additive white Gaussian noise (AWGN) can be added to the channel generated in the RC or by the RC and CE combination. This will remove throughput performance differences due to variations in antenna efficiency between different MIMO systems and solely incorporate effects unique for multi-element antennas, such as correlation and gain imbalance between the antenna elements.

For this study, AWGN was added before the signal from the base station simulator was fed to the fixed measurement antennas of the RC. For the setup utilizing the RC and CE combination, the AWGN was added to the channel after the channel emulator fading.

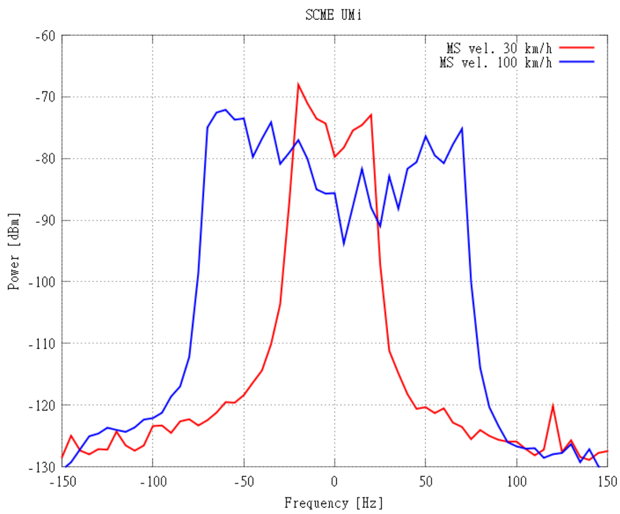

Figure 6. Measured Doppler spectrum for the reverberation chamber and channel emulator setup for two different fading rates (DUT speeds).

V. Reference Antennas

This paper presents results from measurements on three CTIA MIMO reference antennas. These consist of two antenna branches each and they are tuned to LTE frequency band 13 [14]. These are designed to provide “good” (low correlation and high efficiency), “nominal” (moderate correlation and moderate efficiency), and “bad” (high correlation and low efficiency) performance. One of these reference antennas is shown in Figure 7. A commercially available MIMO LTE enabled handset is connected to the two branches of the reference antennas and is used to decode the MIMO signal and enable data bit throughput measurements.

The overall antenna efficiency for the three reference antennas is given in Table I below. Also, the correlation for the same antennas is given in Figure 8. This figure shows a good alignment between the correlation measured for the antennas in the RC and the correlation measured in an anechoic chamber by the manufacturing lab.

Figure 7. One of the reference antennas used for the measurements presented in this paper. An RF enclosure is attached to the antennas, in which the handset used as demodulator is inserted. This will assure shielding of the handset antennas and of device noise coupled to the reference antenna. The device receivers are connected to the reference antenna by short RF cables.

TABLE I. OVERALL ANTENNA EFFICIENCY FOR THE REFERENCE ANTENNAS.

Antenna	Efficiency
CTIA Good	-1.3 dB
CTIA Nominal	-3.1 dB
CTIA Bad	-3.9 dB

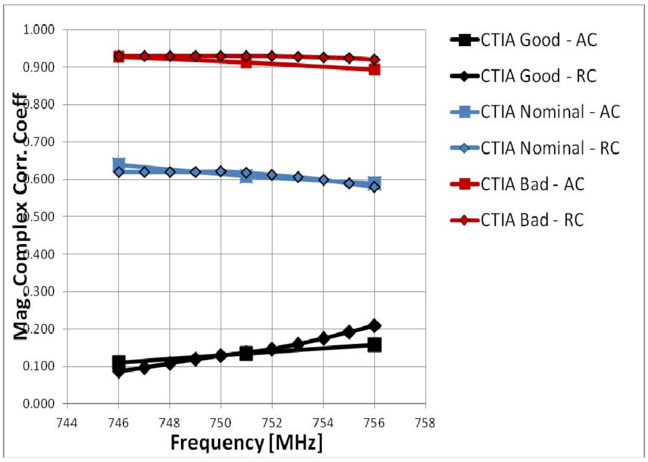

Figure 8. Measured correlation for the CTIA reference antennas. The measured correlation in reverberation chamber aligns well with the reference values provided by the manufacturer (measurements in anechoic chamber).

VI. RESULTS

Data throughput measurements were performed on the reference antennas described in section V. A picture showing the reference antenna setup inside the RC can be found in Figure 9. All results have been collected with the base station simulator configured to emulate open loop spatial multiplexing with 64-QAM modulation. The exact settings used are given in [14].

Figure 10 shows the measured data bit throughput as a function of average power available when using the three reference antennas. It is observed that the expected performance ranking is obtained, with a clear separation between the antennas of about 4-5 dB. Figure 11 shows the results from similar measurements, however, with external AWGN added to the channel. As expected, the difference in performance is smaller in this case, since the effect of the antenna efficiency will be removed in this setup. It is observed that only the high correlation antenna gives a significant difference in throughput performance compared to the other antennas. Comparing this to Figure 10, it can be concluded that the antenna efficiency affects the throughput performance significantly more than the correlation for the Good and Nominal antennas.

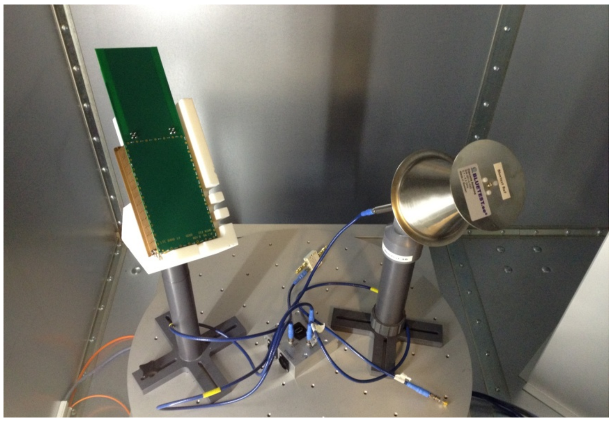

Figure 9. Picture showing the positioning of the reference antenna inside the reverberation chamber.

Figure 11 also shows the measured data bit throughput performance for the same reference antennas when adding AWGN, but when utilizing the RC and CE setup. A somewhat larger difference between the Nominal and Bad antennas is obtained and a small shift in absolute SNR values is observed, but otherwise the results are very similar to what was found for the corresponding case for the basic setup. It is possible to distinguish between the Good and Bad reference antennas, whereas the Nominal antenna shows very little difference compared to the Good antenna.

Furthermore, in Figure 10 and Figure 11 two measurements for each reference antenna are presented. It is observed that the repeatability of the measurements is within 0.5 dB for all cases.

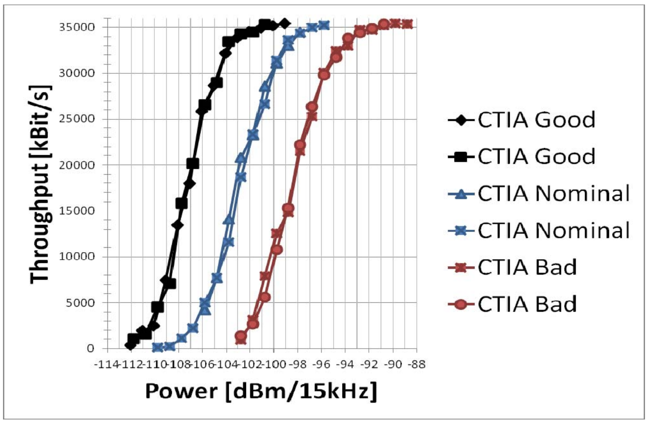

Figure 10. Results from data throughput measurements comparing the “good”, “nominal” and “bad” reference antennas (different colors) for open loop spatial multiplexing and 64-QAM modulation. Results for two repeated measurements for each antenna are shown in the figure (same color). The measurements have been performed with the basic RC measurement setup.

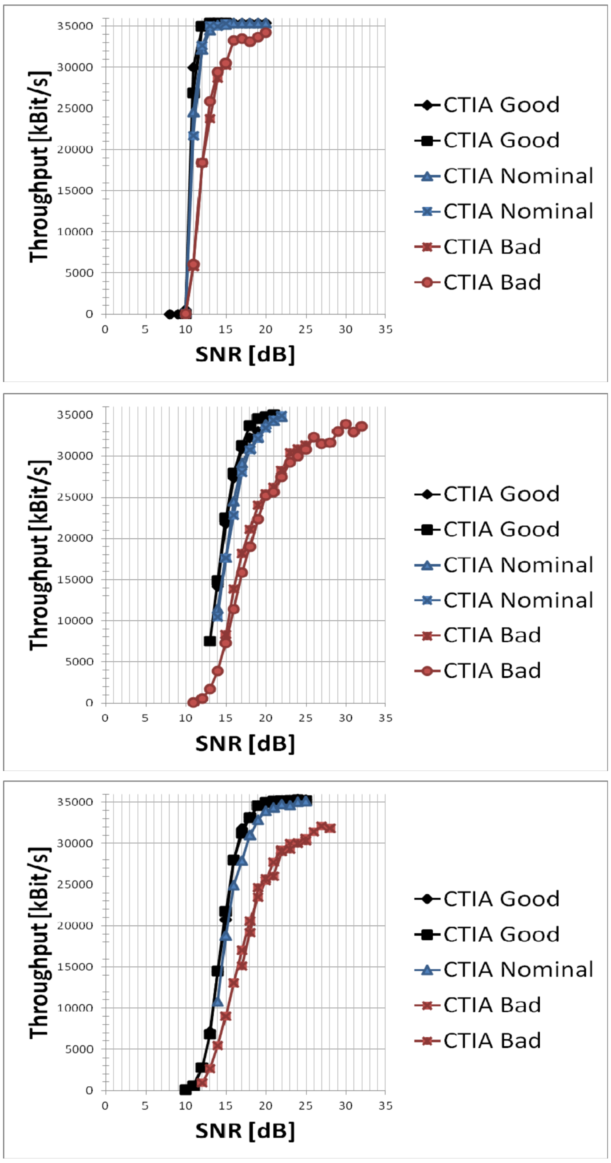

Figure 11. Results from data throughput measurements for the basic RC setup (top) and the RC and CE setup, with the CE emulating the temporal properties of the SCME UMi (middle) and UMa (bottom) channel model.

VII. Conclusion

This paper presents results from data throughput measurements in the reverberation chamber on commercial available units combined with a set of multi-element reference antennas with known performance. The correlation these reference antennas was measured in a reverberation chamber and the result aligned well with reference values. It was further shown that the expected performance ranking can be obtained by performing data throughput measurements in a reverberation chamber. By adding additive white Gaussian noise to the signal it was possible to study effects on data throughput performance solely due to correlation and gain imbalance. It was concluded that the efficiency had the biggest impact when the correlation is low, with the correlation being an important parameter for highly correlated antennas only.

The basic reverberation chamber setup was also extended to incorporate a channel emulator. This enabled testing with other temporal properties, keeping the spatial properties the same as for the basic setup. The data throughput was measured for the reference antennas and similar results as for the basic setup were observed, however, with a small shift in absolute values.

References

[1] P.-S. Kildal, X. Chen, C. Orlenius, M. Franzén, C. Lötbäck Patané, "Characterization of Reverberation Chambers for OTA Measurements of Wireless Devices: Physical Formulations of Channel Matrix and New Uncertainty Formula," IEEE Transactions on Antennas and Propagation, Vol. 60, No. 8, pp. 3875-3891, Aug. 2012.

[2] K. Rosengren and P. S. Kildal, "Radiation efficiency, correlation, diversity gain and capacity of a six-monopole antenna array for a MIMO system: theory, simulation and measurement in reverberation chamber," IEE Proceedings - Microwaves, Antennas and Propagation, Vol. 152, pp. 7-16, 2005. See also Erratum published in August 2006.

[3] M. Andersson, A. Wolfgang, C. Orlenius, J. Carlsson, "Measuring Performance of 3GPP LTE Terminals and Small Base Stations in Reverberation Chambers", Chapter 12 of "Long Term Evolution: 3GPP LTE Radio and Cellular Technology", CRC Press, 2009.

[4] P.-S. Kildal and K. Rosengren, "Correlation and capacity of MIMO systems and mutual coupling, radiation efficiency and diversity gain of their antennas: Simulations and measurements in reverberation chamber", IEEE Communications Magazine, vol. 42, no. 12, pp. 102-112, Dec. 2004.

[5] X. Chen, P. S. Kildal, J. Carlsson, and J. Yang, "MRC diversity and MIMO Capacity Evaluations of Multi-Port Antennas Using Reverberation Chamber and Anechoic Chamber," to appear in IEEE Transaction on Antennas and Propagation, available as early access on IEEE Xplore, Nov. 2012.

[6] P. S. Kildal, A. Hussain, X. Chen, C. Orlenius, A. Skårbratt, J. Åsberg, T. Svensson, and T. Eriksson, "Threshold Receiver Model for Throughput of Wireless Devices with MIMO and Frequency Diversity Measured in Reverberation Chamber," IEEE Antennas and Propagation Wireless Letters, vol. 10, pp. 1201-1204, October 2011.

[7] X. Chen, P. S. Kildal, C. Orlenius, and J. Carlsson, "Channel Sounding of Loaded Reverberation Chamber for Over-the-Air Testing of Wireless Devices: Coherence Bandwidth Versus Average Mode Bandwidth and Delay Spread," IEEE Antennas and Wireless Propagation Letters, vol. 8, pp. 678-681, 2009.

[8] X. Chen, P. S. Kildal, and S. H. Lai, "Estimation of Average Rician K-Factor and Average Mode Bandwidth in Loaded Reverberation Chamber," IEEE Antennas and Wireless Propagation Letters, vol. 10, pp. 1437-1440, 2011.

[9] C. Lötbäck Patané, M. Franzén, C. Orlenius, "Analysis and Improvement of Reverberaiton Chamber Method for Characterization of Small and Terminal Antennas", EuCAP 2011, April 2011.

[10] P.-S. Kildal, C. Orlenius, J. Carlsson, "OTA Testing in Multipath of Antennas and Wireless Devices with MIMO and OFDM," Proceedings of the IEEE, Vol. 100, No. 7, pp. 2145-2157, July 2012.

[11] P. S. Kildal and K. Rosengren, "Correlation and capacity of MIMO systems and mutual coupling, radiation efficiency, and diversity gain of their antennas: simulations and measurements in a reverberation chamber," IEEE Communications Magazine, vol. 42, pp. 104-112, 2004.

[12] J. Åsberg, A. Skårbratt, C. Orlenius, J. Byun, S. Park, P.-S. Kildal, "State-of-the-Art Measurements of LTE Terminal Antenna Performance Using Reverberation Chamber", EuCAP 2011, April 2011.

[13] C. Orlenius, C. Lötbäck Patané, A. Skårbratt, J. Åsberg, M. Franzén, "Analysis of MIMO OTA Measurements for LTE Terminals Performed in Reverberaiton Chamber", EuCAP 2012, March 2012.

[14] I. Szini, A. Scannavini, "Measurement results analysis on CTIA MIMO 2x2 Reference Antennas produced by Satimo", CTIA MOSG120504, May 2012.

[15] S. Prather, "Inter-Lab/Inter-Technique OTA Performance Comparison Testing for MIMO Devices", CTIA MOSG120521R4, August 2012.